Effect of fluorine functional groups on surface and mechanical interfacial properties of epoxy resins

Fan-Long Jin [a], Hak-Yong Kim [b], Soo-Jin Park [c],*

[a] Department of Chemical Engineering, Jilin Institute of Chemical Technology, Jilin City 132022, PR China
[b] Department of Textile Engineering, Chonbuk National University, Chonju 560-756, South Korea
[c] Department of Chemistry, Inha University, Nam-gu, Incheon 402-751, South Korea

Abstract

To improve the surface and mechanical interfacial properties of epoxy resins, fluorine-containing epoxy resin (FEP) was prepared and blended with a commercially available tetrafunctional epoxy resin (TGDDM). As a result, when the fluorine content increased, the total surface energy of TGDDM/FEP blends was gradually decreased, while the water repellency of the blends was increased. The glass transition temperature and thermal stability factors of the blends showed maximum values at 20–40 wt% FEP compared with neat TGDDM epoxy resins. And the mechanical interfacial properties of the blend specimens were significantly increased with increasing the FEP content, which could be attributed to the intermacromolecular interactions in the cured TGDDM/FEP blends. These results indicate that the water repellency and toughness improvements have been achieved without significantly deterioration of the thermal properties in the TGDDM/FEP blends.
© 2006 Elsevier B.V. All rights reserved.

Keywords: Epoxy resin; Fluorine; Glass transition temperature; Thermal stability; Fracture toughness

1. Introduction

The tetrafunctional epoxy resins, 4,4′-tetradiglycidyl diaminodiphenyl methane (TGDDM), are widely used as matrix materials in carbon fibers-reinforced structural polymer composites in the aircraft and aerospace industries [1]. However, TGDDM have major drawbacks of brittleness and high level of moisture absorption, which constrains their many end-use applications. Recently, many attempts have been made to overcome these problems [2].

The use of fluorinated monomers and oligomers for modification of epoxy resins is attractive due to the unique characteristics given by the presence of fluorine, such as outstanding chemical resistance, low coefficient of friction, low dielectric constant, low water absorption, and broad use temperature [3–6]. Griffith [7] and Maruno and Nakamura [8] first reported the synthesis of fluorine-containing epoxy resins. The cure and transition behaviors of highly and partially fluorinated epoxy resins are investigated by Twardowski and Geil [9] and Dammont and Kwei [10]. Kasemura et al. showed the fluorinated aromatic compounds have been added to TGDDM epoxy resins/4,4′-diaminodiphenyl sulfone (DDS) systems in order to reduce moisture sensitivity [11]. In another report, the surface modification of epoxy resins has been made with fluorine-containing methacrylic ester copolymers for the purpose of improving oil and water repellency [12]. Misaki et al. studied various kinds of aromatic and aliphatic glycidyl compounds are used as a modifier to improve the fracture properties of 4,4′-diaminodiphenyl methane (DDM) cured epoxy resins [13]. Recently, authors reported the synthesis and properties of a new fluorine-containing epoxy resin [14].

Thus, it is more interesting that the introduction of the fluorine-containing epoxy resins into the commercially available tetrafunctional epoxy resins to investigate the effect of fluorine content on the physicochemical and mechanical interfacial properties of epoxy blends. In this study, the surface properties, thermal stabilities, and mechanical interfacial properties of fluorine-containing epoxy resin, i.e., 4,4-diglycidylether benzotrifluoride (FEP), modified tetrafunctional epoxy resins/DDM systems are investigated by using the

* Corresponding author. Tel.: +82 42 860 7234; fax: +82 42 861 4151.
E-mail address: sjpark@inha.ac.kr (S.-J. Park).

Table 1
XPS surface concentrations for TGDDM/FEP blends

TGDDM/FEP	C (%)	F (%)	O (%)	N (%)
100:0	79.6	0	12.8	7.6
80:20	78.3	1.0	14.6	6.1
60:40	76.1	1.9	16.2	5.8
40:60	74.5	3.1	17.3	5.1
20:80	70.9	4.3	20.5	4.3
0:100	67.8	5.6	23.2	3.4

sessile drop method, thermogravimetric analysis (TGA), dynamic mechanical analysis (DMA), a universal test machine (UTM), and scanning electron microscope (SEM).

2. Results and discussion

2.1. Surface properties

Surface composition of TGDDM/FEP blends was investigated by XPS measurements. The results of carbon, fluorine, oxygen, and nitrogen atomic compositions for the blends are given in Table 1. The fluorine content of the blends increases with increasing the FEP content.

The studies on surface composition and structure in multicomponent polymer systems have been conducted because of the surface composition significantly affect the bulk properties of polymer blends [15]. And fluorochemicals are commonly applied to reduce surface free energy and decrease wetting on many types of surfaces [16]. To study an effect of fluorine content on the surface properties of TGDDM/FEP blends, a change of the surface free energy was investigated by contact angle measurements.

The contact angles for TGDDM/FEP blends were measured for three testing liquids, i.e., glycerin, diiodomethane, and deionized water. Fig. 1 shows the contact angles of water on the blends as a function of FEP content. As observed, the sessile drop water contact angles for the blends increase with increasing the FEP content, which is due to an increase of
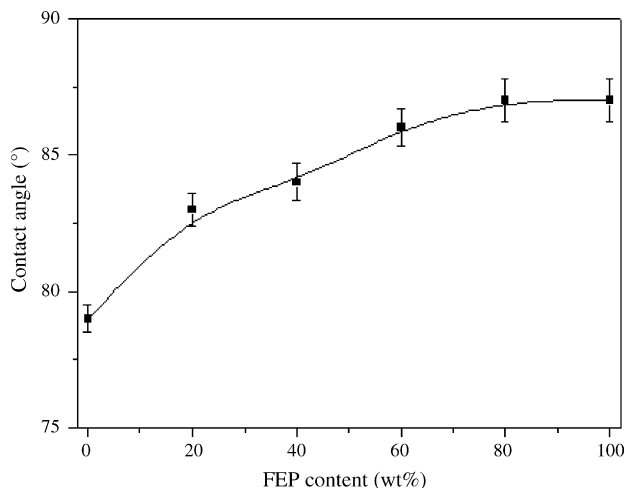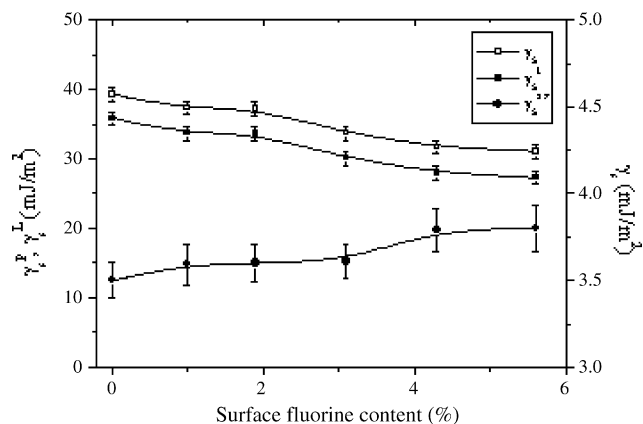

Fig. 2. Variation of surface free energies for TGDDM/FEP blends as a function of surface fluorine content.

the polar fluorine groups of the blends per unit surface area [17,18]. This result indicates that the hydrophobic property, i.e., water repellency, of the blends is increased as the fluorine content increased. Fitch et al. has been observed a similar phenomenon in fluorine-containing polyether systems [4].

The surface free energy or surface tension (γ_S) of a solid can be expressed by the sum of the London dispersive (γ_S^L) and specific (γ_S^{SP}) components since they have been introduced by Fowkes [19]:

$$\gamma_S = \gamma_S^L + \gamma_S^{SP} \tag{1}$$

where γ_S is the London attraction of van der Waals' forces as a dispersive or non-polar force (in mJ m^{-2}) and γ_S^{SP} is all other non-dispersive components of intermolecular interactions (in mJ m^{-2}).

The surface free energy of TGDDM/FEP blends as a function of surface fluorine content is shown in Fig. 2. The total surface free energy of the blends gradually decreases with increasing the surface fluorine content, which is mainly due to lower London-dispersive component, while the specific component is increased. This can be attributed to an increase of the polar fluorine groups per unit surface area in the TGDDM/FEP blends, as mentioned [17,18].

2.2. Dynamic mechanical analysis

Glass transition temperature of TGDDM/FEP blends was determined by using DMA in a wide temperature range 50–250 °C at a heating rate of 5 °C min^{-1}. Fig. 3 shows the temperature dependence of the loss factor (tan δ) for the cured neat TGDDM epoxy resins and blend specimens. From the DMA spectra, the blends show a single relaxation as the FEP content increased, which indicate that the blends were homogeneous and that any phase separation did not occur. The glass transition temperature (T_g) value was assumed as a maximum of tan δ curve. The obtained T_g values of the blends are shown in Table 2. From the result, it can be confirmed that the T_g values of blends containing 40 wt% FEP was similar to that of neat TGDDM epoxy resins. This is attributed to the
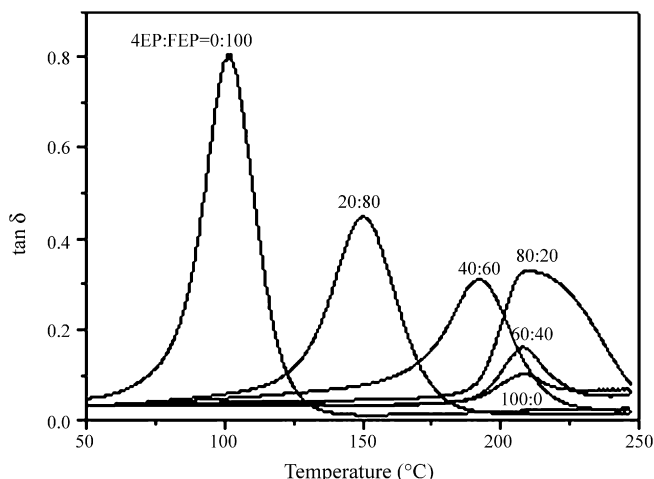

Fig. 1. The contact angles of water for TGDDM/FEP blends as a function of FEP content.

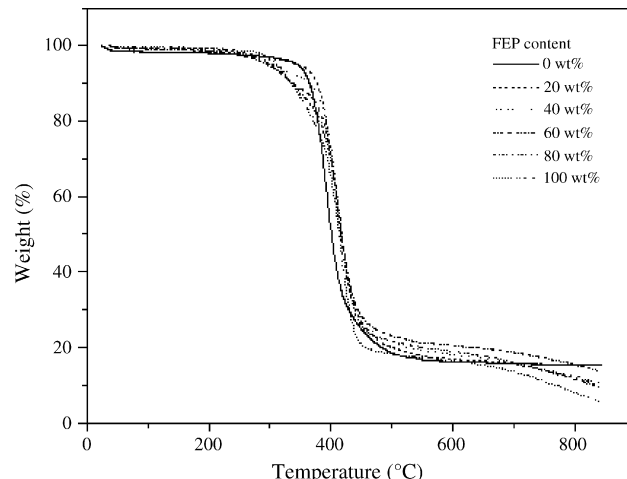Fig. 3. Dynamic mechanical spectra of TGDDM/FEP blends as a function of FEP content.

Table 2
Glass transition temperature (T_g) of the cured TGDDM/FEP blends

TGDDM/FEP	T_g (°C)
100:0	209
80:20	210
60:40	208
40:60	193
20:80	150
0:100	102

relatively large volume of fluorine compared with hydrogen [17]. Whereas above this content, the T_g value of the blends decreases with increasing the FEP content. The decreased T_g of the blends indicates that the introduction of trifluoromethyl (CF$_3$) groups sharply reduces confinement of internal network junctions at high fluorine content [14].

2.3. Thermal properties

The use of thermogravimetric analysis (TGA) with the thermal dynamic measurements and their thermograms can provide the characteristics of blends and serves as the evidence of the blend formation [18]. The thermal degradation behaviors of TGDDM/FEP blends was studied with TGA at a heating rate of 10 °C min^{-1} in a nitrogen atmosphere and the TGA thermograms of the blends are shown in Fig. 4. Thermal stability factors, including the initial decomposed temperature (IDT; 5% weigh loss), the temperatures of maximum rate of degradation (T_{max}), and the decomposition activation energy (E_d), of the blends were determined from the TGA thermo-grams [20]. And the E_d values of the blends were calculated from TGA curves by the integral method of Coats and Redfern's equation, as follows [21]:

$$\ln \frac{\alpha}{T^2} = \ln \frac{AR}{\beta E_d} \left(\frac{1 - 2RT}{E_d} \right) - \frac{E_d}{RT} \qquad (2)$$

Fig. 4. TGA thermograms of TGDDM/FEP blends as a function of FEP content.

where α is the decomposed fraction, T the temperature of maximum rate of degradation (K), A the Arrhenius pre-expo-nential factor (min^{-1}), β the heating rate (K min^{-1}), and R is the gas constant (8.3145 J mol^{-1} K^{-1}).

The thermal stability factors of the blends are summarized in Tables 3 and 4. As a result, the IDT and E_d of the blends increase with FEP content up to 20 wt% FEP. The increased thermal stability can be explained by intermacromolecular interactions in the TGDDM/FEP blends.

The partial spectra of TGDDM/FEP blends in the wavenumber range from 3100 to 3800 cm^{-1} is shown in Fig. 5. The wide distribution of hydrogen-bonded hydroxyl stretching vibrations can be reflected from the very broad bands. The center of the hydroxyl band for the blends is shifted to lower frequency with increasing the FEP content, as shown in Fig. 5. The low-frequency shift indicates that the hydrogen bonding interactions are formed between the hydroxyl group of TGDDM and the carbonyl or hydroxyl group of FEP in the blends of TGDDM/FEP [22].

And above this content, the thermal stabilities of the blends decrease as the FEP content increased. From the DMA and TGA results, it can be confirmed that the blends containing 20–40 wt% FEP still possess excellent glass transition temperature and thermal stability as well as neat TGDDM epoxy resins.

2.4. Mechanical interfacial properties

The critical stress intensity factor (K_{IC}) of TGDDM/FEP blends was determined using SEN test according to the

Table 3
Thermal stability factors of TGDDM/FEP blends as a function of FEP content

TGDDM/FEP	IDT (°C)	T_{max} (°C)
100:0	345	393
80:20	346	408
60:40	304	412
40:60	296	414
20:80	303	418
0:100	292	417

Table 4
Decomposition activation energy (E_d) of TGDDM/FEP blends calculated from TGA thermograms

TGDDM/FEP	$\ln(\alpha/T^2)$	$(-1/T)$	E_d/RT_S^2	E_d (kJ mol^{-1})
100:0	−43.2	−2.8482	0.0356	132
	−13.2	−1.4023		
	16.7	−0.0918		
	46.7	0.2678		
80:20	−58	−2.9201	0.0363	140
	−28.3	−2.1182		
	2	−0.5801		
	31.9	0.1876		
60:40	−61.9	−2.4384	0.0300	117
	−31.8	−1.9064		
	−2	−0.6779		
	28.2	0.1539		
40:60	−64	−2.1163	0.0262	103
	−34.1	−1.6919		
	−4.3	0.6678		
	25.8	0.1514		
20:80	−67.6	−2.0186	0.0253	100
	−37.5	−1.5369		
	−7.4	−0.6387		
	22.4	0.2173		
0:100	−66.7	−1.9087	0.0256	101
	−36.9	−1.3488		
	−6.7	−0.4960		
	23	0.3677		

relationship (3), which was originally developed as a standard test for plane strain fracture toughness of the materials [23,24]:

$$K_{IC} = PBW^{1/2}Y \tag{3}$$

where P is the rupture force (kN), B the specimen thickness (cm), W the specimen width (cm), and Y is the geometrical factor.

Fig. 6 shows the relationship between the K_{IC} values of the blends and the FEP content. As observed, the neat epoxy resins are brittle, with a 0.65 MPa m$^{1/2}$. The K_{IC} values of the blends
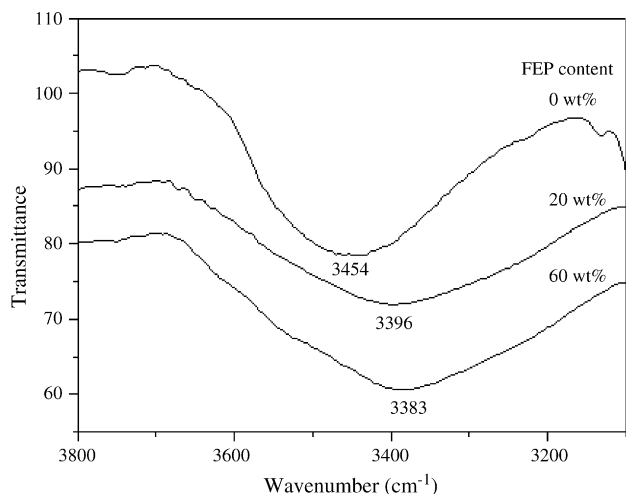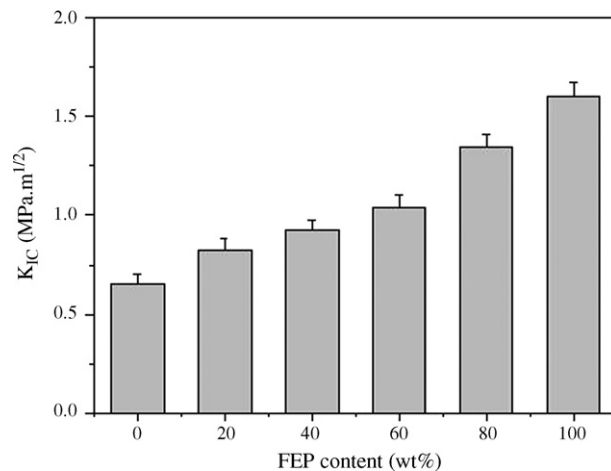

Fig. 6. Effect of FEP content on the K_{IC} for TGDDM/FEP blends.

are significantly increased as the FEP content increased. This can be attributed to the intermacromolecular interactions, such as hydrogen bonding, between the hydroxyl group of TGDDM and the carbonyl or hydroxyl group of FEP in the TGDDM/FEP blends [22,25]. The result is also due to the increased flexibility of the chain induced by CF$_3$ groups in the blends [14]. It is important to point out that the toughness improvement has been achieved without significantly decrease in the thermal properties.

Between the γ_S^{SP} and the K_{IC} have a good linearity, as shown in Fig. 7. This is a consequence of the increase of the specific component of surface free energy in the blends, resulting in the increased intermacromolecular interactions in the TGDDM/FEP blends [26].

The fracture behaviors of TGDDM/FEP blends can be explained in terms of morphology observed by SEM. Fig. 8(a) shows SEM micrograph of the neat epoxy resins, exhibits a regulative cracks in the fracture surface, indicating a brittle fracture surface, which accounts for its poor fracture properties. In contrast, the micrographs of the blends show tortuous cracks
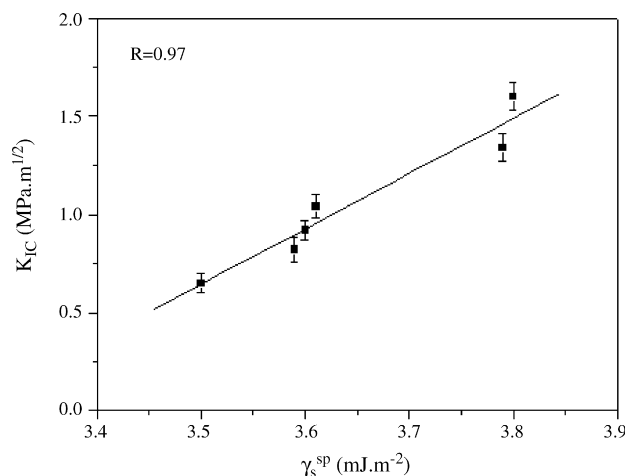

Fig. 5. Shift of IR peak for hydroxyl absorption in TGDDM/FEP blends.

Fig. 7. Dependence of the critical stress intensity factor on the specific component of surface free energy for TGDDM/FEP blends (R is the coefficient of regression).
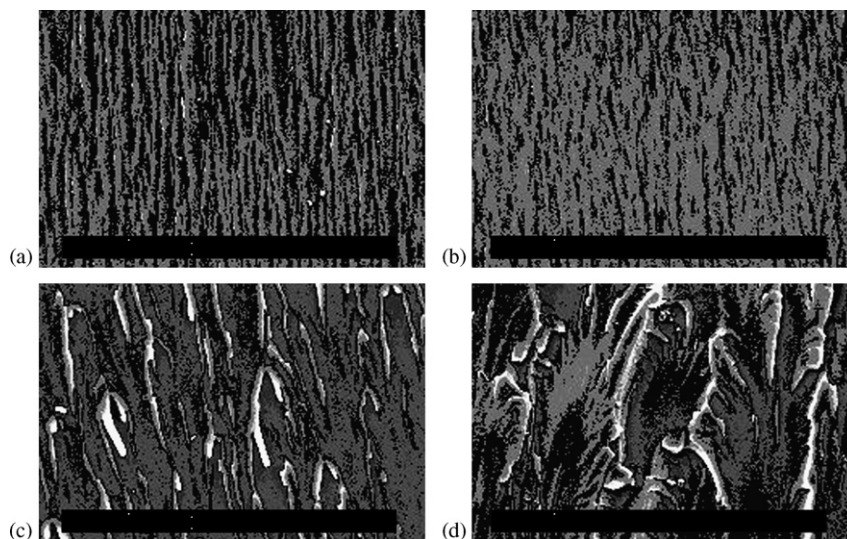
Fig. 8. SEM micrographs of TGDDM/FEP blends after K_{IC} tests: (a) 100:0, (b) 60:40, (c) 20:80, and (d) 0:100 (magnification of 1000×).

and exhibit many ridges, indicating a reinforced morphology, as shown in Fig. 8(b)–(d) [27].

3. Conclusions

The surface and bulk properties of tetrafunctional epoxy/fluorine-containing epoxy blends cured with DDM as a curing agent were investigated. The results indicated that the total surface free energy of TGDDM/FEP blends was gradually decreased with increasing the fluorine content. This was because of an increase of the polar fluorine groups of the blends per unit surface area. The blends showed higher bulk properties compared with neat TGDDM. The glass transition temperature and thermal stability factors of the blends show maximum values at 20–40 wt% FEP content. And the fracture toughness of the cured specimens was increased as the FEP content increased, which was due to the hydrogen bonding interactions in the TGDDM/FEP blends. The K_{IC} values of the blends were also increased with increasing the specific component of surface free energy.

According to these results, it is confirmed that the fluorine-containing epoxy resin was an excellent modifying agent for TGDDM epoxy resins, because of the increase the water repellency and toughness without significantly deterioration of the thermal properties in the TGDDM/FEP blends.

4. Experimental

4.1. Materials

Epoxy resin used in this study was 4,4′-tetradiglycidyl diaminodiphenyl methane (TGDDM, supplied from LG Chem. of Korea), which had an epoxide equivalent weight (EEW) of 110–130 g equiv.$^{-1}$, a density of about 1.17 g cm^{-3} at 25 °C, and a viscosity of about 14000 cps at 25 °C. Fluorine-containing epoxy resin, 4,4-diglycidylether benzotrifluoride (FEP), was synthesized in our lab scale [14]. 4,4′-Diamino-

diphenyl methane (DDM) purchased from Aldrich Chem. was selected as a curing agent. The chemical structures of TGDDM, FEP, and DDM are shown in Fig. 9.

4.2. Synthesis of the epoxy resin

4-Chlorobenzotrifluoride (27.1 g, 0.15 mol), glycerol diglycidylether (30.6 g, 0.15 mol), hydroquinone (0.12 g), and pyridine (0.28) were placed in a 500 ml four-neck round flask equipped with mechanical stirrer, thermometer, and reflux condenser. The mixture was reacted at 30 °C for 24 h. After the reaction was completed, the crude product was dissolved in toluene and filtered, then toluene and unreacted reactant were distilled off at 100 °C and 70 kPa. Finally, the product was dried
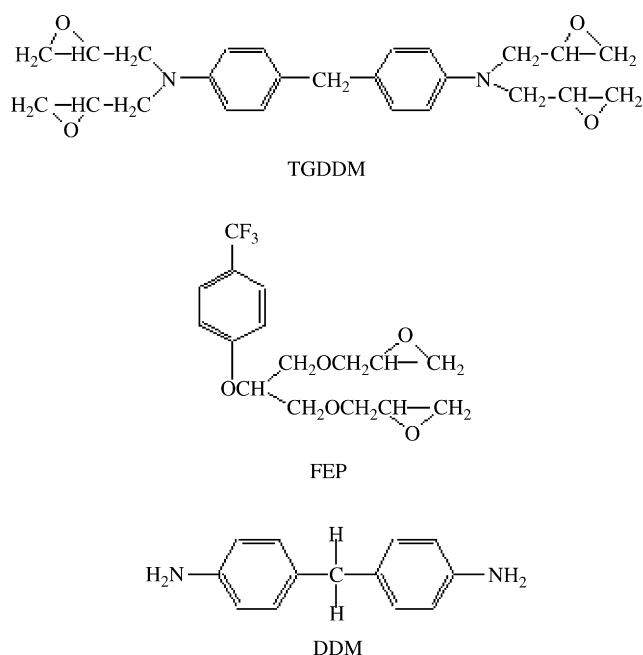

Fig. 9. Chemical structures of the materials used.

in a vacuum oven at 100 °C for 8 h. The obtained epoxy resin was a viscous liquid and the yield was 81%. The EEW of the epoxy resin was 172 g equiv.$^{-1}$.

FT-IR (KBr, ν (cm^{-1})): 1103 (CF$_3$ group), 910, 851 (epoxide group).

^{1}H NMR (acetone-d_6): δ 7.3–7.5 (4H, aromatic H), 2.8–3.2 (3H, epoxide group).

^{13}C NMR (acetone-d_6): δ 134–127.7 (aromatic ring), 127.5 (CF$_3$), 70.6, 50.5, 43.3 (epoxide group).

^{19}F NMR (acetone-d_6): δ −62.0 (3F).

4.3. Sample preparation

The overall amino-hydrogen to epoxy ratio was 1. TGDDM and FEP were mixed at a weight ratio of 100:0 to 0:100. TGDDM and FEP were mixed in an oil bath at 90 °C and then DDM was added to the epoxy mixture. The mixtures were completely mixed by magnetic stirring bar and then degassed in a vacuum oven to eliminate air bubbles. The preparation of the specimens for thermal and mechanical tests was as follows: bubble-free mixtures were poured into a stainless mold and cured at 110 °C for 1 h, 140 °C for 2 h, and finally postcured at 170 °C for 1 h in a convection oven. The specimens were cut to suitable dimensions for the thermal and mechanical tests.

4.4. Characterization and measurements

FT-IR measurement was performed with a Bio-Rad Co. digilab FTS-165 spectrometer by using KBr pellets. ^{1}H NMR, ^{13}C NMR, and ^{19}F NMR spectra were obtained by BRUKER Co. DRX300 spectrometer operating at 300 MHz using acetone-d_6 as solvent.

The surface composition of TGDDM/FEP blends was measured using an X-ray photoelectron spectroscopy (VG Scientific ESCA LAB MK-II spectrometer).

The surface free energy of the blends was determined at 20 ± 1 °C using a sessile drop method on a Surface & Electro-Optic Co. SEO 300A. Three different wetting liquids, i.e., glycerin, deionized water, and diiodomethane, were selected. For each sample, every calculated contact angle was an average of 10 measurements with a standard deviation below 1°.

The temperature dependence of the loss factor (tan δ) of various samples was measured using a dynamic mechanical analyzer (RDS-II, Rheometrics Co.) in a frequency of 1 Hz and the temperature range from 50 to 250 °C at a heating rate of 5 °C min^{-1}.

The thermal stability of the cured samples was investigated with a du Pont TGA-2950 analyzer from 30 to 850 °C at a heating rate of 10 °C min^{-1} under the condition of nitrogen atmosphere.

The critical stress intensity factor (K_{IC}) was characterized by single edge notched (SEN) testing in three-point bending flexure. The three-point bending test was conducted on a universal testing machine (Instron Model 1125) according to the ASTM D 256-73.

All mechanical properties were obtained by using the five specimens for each condition. The fractured surfaces were examined by scanning electron microscope (SEM, JEOL JXA 840A).

References

[1] C.A. May, Epoxy Resins, Chemistry and Technology, Marcel Dekker Inc., New York, 1988.
[2] S.J. Park, F.L. Jin, J.R. Lee, Mater. Sci. Eng. A 374 (2004) 109–114.
[3] E.S. Wilks, Industrial Polymers Handbook, Products, Processes, Applications, Wiley–VCH, New York, 2001.
[4] J.W. Fitch, E. Bucio, L. Martinez, J. Macossay, S.R. Venumbacka, N. Dean, D. Stoakley, P.E. Cassidy, Polymer 44 (2003) 6431–6434.
[5] S. Turri, M. Scicchitano, C. Tonelli, J. Polym. Sci. Polym. Chem. 34 (1996) 3263–3275.
[6] S. Matuszczak1, W.J. Feast, J. Fluorine Chem. 102 (2000) 269–277.
[7] J.R. Griffith, Chemtech 12 (1982) 290–293.
[8] T. Maruno, K. Nakamura, J. Appl. Polym. Sci. 42 (1991) 2141–2148.
[9] T.E. Twardowski, P.H. Geil, J. Appl. Polym. Sci. 41 (1990) 1047–1054.
[10] F.R. Dammont, T.K. Kwei, J. Polym. Sci. Pt. A-2 5 (1967) 761–769.
[11] T. Kasemura, Y. Oshibe, H. Uozumi, S. Kawai, Y. Yamada, T. Yamamoto, J. Appl. Polym. Sci. 47 (1993) 2207–2216.
[12] L. Matisová-Rychlá, J. Rychlý, J. Vercu, L. Audouin, A. Tcharkhtchi, I. Janigova, J. Appl. Polym. Sci. 53 (1994) 1375–1384.
[13] T. Misaki, T. Hirohata, M. Yoshii, J. Appl. Polym. Sci. 37 (1989) 2617–2625.
[14] J.R. Lee, F.L. Jin, S.J. Park, J.M. Park, Surf. Coat. Technol. 180/181 (2004) 650–654.
[15] S.Y. Liu, M. Jiang, C.M. Chan, L.T. Weng, Macromolecules 34 (2001) 3802–3804.
[16] R.R. Thomas, K.G. Lloyd, K.M. Stika, L.E. Stephans, G.S. Magallanes, V.L. Dimonie, E.D. Sudo, M.S. El-Aasser, Macromolecules 33 (2000) 8828–8841.
[17] S.J. Park, H.S. Kim, F.L. Jin, J. Colloid Interf. Sci. 282 (2005) 238–240.
[18] S.T. Lin, S.K. Huang, J. Polym. Sci. Polym. Chem. 34 (1996) 869–884.
[19] F.M. Fowkes, J. Phys. Chem. 66 (1962) 382–1382.
[20] F.L. Jin, S.J. Park, J. Polym. Sci. Polym. Phys. 44 (2006) 3348–3356.
[21] A.W. Coats, J.W. Redferm, J. Polym. Sci. Polym. Lett. 3 (1965) 917–920.
[22] H. Lü, S. Zheng, J. Polym. Sci. Polym. Phys. 43 (2005) 359–367.
[23] S.J. Park, F.L. Jin, J.R. Lee, Macromol. Chem. Phys. 205 (2004) 2048–2054.
[24] S.J. Park, M.K. Seo, J.R. Lee, D.R. Lee, J. Polym. Sci. Polym. Chem. 39 (2001) 187–195.
[25] H.L. Huang, S.H. Goh, D.M.Y. Lai, A.T.S. Wee, C.H.A. Huan, J. Polym. Sci. Polym. Chem. 42 (2004) 1145–1153.
[26] S.J. Park, Y.S. Jang, J. Colloid Interf. Sci. 237 (2001) 91–97.
[27] I. Blanco, G. Cicala, C.L. Faro, A. Recca, J. Appl. Polym. Sci. 89 (2003) 268–273.